Experimental Study on Developing Process of Local Scour around a Vertical Cylinder

Tomonao Kobayashi[1]   and   Kenji Oda[2]

ABSTRACT

Time evolution of scoured seabed profiles around a vertical slender cylinder under waves has been investigated by means of laboratory experiments. The characteristics of the scoured bed profiles on the developing process is discussed considering the flow features. The local scoured bed profiles are classified with the location of the maximum scoured point. And the developing scouring process of each classified type is discussed. We found that for each scour type, the scoured bed retains a similar profile during its whole developing process. The ultimate scour depth on the vicinity of the cylinder surface is related to the Keulegan-Carpenter number, and it is independent of the sand bed condition.

1. INTRODUCTION

Local scouring is an important factor to consider when the stability of offshore and onshore structures is analyzed, and different aspects of this have already been investigated by various researchers. Among them, Well and Sorensen (1970) based on laboratory experiments found relations of the ultimate scour depth to the Shields number, Reynolds number, etc. Sumer *et al.* (1992), also based on laboratory tests, proposed the scour depth as a function of the Keulegan-Carpenter (K.C.) number on the live bed, *i.e.* the bottom with continuous sediment motion. Nishizawa and Sawamoto (1988) studied the flow around a vertical slender cylinder under waves using flow visualization techniques, and reported relations between the flow characteristics and the K.C. number. Kobayashi (1993) measured in the laboratory the velocity distributions around a cylinder near the bed on both flat bottom and scoured bed, and discussed about the effect of the scoured seabed configuration on the vortex behavior near the bed around the cylinder.

In most of the available literature about the local scouring phenomenon around a vertical slender cylinder under waves, only the ultimate scoured bed

---

[1]Research Associate, Department of Civil Engineering, Tokyo Rika University, 2641 Yamazaki, Noda city, Chiba 278, Japan.
[2]Tokyu Construction Co., Tokyo, Japan.

TABLE 1. Incident Wave Conditions at The Cylinder

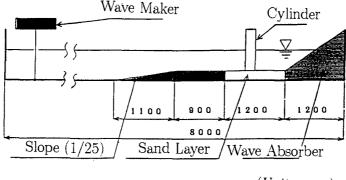| Wave Height	H	13~60mm
Wave Period	T	1.3~3.0s
Water Depth	h	120mm
K.C. number	K.C.	$3.95 \sim 30.0$

is considered. To recognize this physical phenomenon, however, the developing process of the local scouring should also be studied.

The intent of the present study is therefore to recognize the characteristics of the developing process of the local scour around a cylinder under waves. For this purpose, first, the scoured bed profiles are classified into several typical scour types. Then, for each scour type the characteristics of the time evolution of the scoured bed profiles are discussed by considering the flow features on the bed. Finally, relations of the ultimate scour depth to the typical parameters are also discussed.

2. EXPERIMENTAL APPARATUS

Figure 1 shows a sketch of the wave flume employed. The size of this flume is 8 m in length, 300 mm in width and 150 mm in height. Both flume lateral walls are made of glass to facilitate the observations. Part of the bottom flume was lifted to make a movable bed, and in the transition from the bottom flume to the sand bed a slope was located. The bottom of a cylinder was inserted on the movable bed. To classify the local scoured bed profiles, a cylinder of 30 mm diameter was used for the experiments, and in the case of the time evolution of the local scouring experiments, the cylinder diameter was 22 mm.

The wave conditions at the cylinder are shown in Table 1. The maximum

(Unit : mm)

FIG. 1.   Side View of Flume

TABLE 2.   Sand Type

Sand type (Collected place)	Diameter d_{50} (mm)	Specific weight s
Toyoura	0.17	2.569
Toyoumi	0.16	2.556
Makuhari	0.20	2.525
Komesu	0.43	2.695
Oarai	0.17	2.643

velocity at the bottom, that is used to calculate the value of the K.C. number, is evaluated from the wave conditions shown in Table 1 by applying the linear wave theory. During the experiments, the five types of sand shown in Table 2 were employed, and the waves were produced until the scoured bed was considered to be almost stable.

All experiments were done under the clear water condition, because in this way, only the sand near the cylinder moves due to the secondary flow driven by the existence of the cylinder. Hence the characteristics of the flow near the bed around the cylinder are easy to recognize. This is an important matter to understand the local scouring process.

Scoured bed profiles were measured in two dimensions with a sand profile meter.
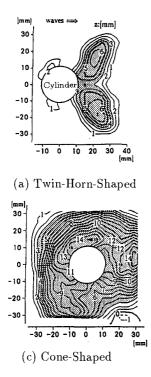
3. CLASSIFICATION OF SCOUR TYPE

The contour maps of the bed profiles around the cylinder in Fig. 2 show typical scour types that were observed during the experiments performance. In this figure, hatched areas indicate scoured regions. The Twin-Horn-Shaped and Cone-Shaped scoured bed profiles in this figure have already been studied by Nishizawa and Sawamoto (1988) among others. In this study, we found the following same results as those reported by them: in the Twin-Horn-Shaped bed the lee side of the cylinder is scoured, and in the case of the Cone-Shaped bed the scouring takes mainly place around the cylinder. When we were performing the experiments, we observed an additional scoured bed type as shown in Fig. 2 (b). Here, both the lee side of the cylinder and the vicinity of the cylinder are scoured. We classified this scour type as Transient-Shaped scoured bed. In this study therefore the scour bed profiles are classified into the categories: Twin-Horn-Shaped, Transient-Shaped and Cone-Shaped bed profiles. An example of each of these bed profiles is shown in Fig. 2. The classification mentioned above, based on the scoured bed profiles, is rather subjective. So, to classify objectively the scour types we introduce the use of the location of maximum scoured point.
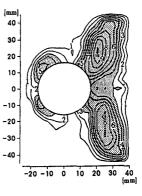
Figure 3 shows the distribution of the maximum scoured points of all experimental cases. In this figure, the marks indicate the scour types classified with the scoured bed profile. Here, the Twin-Horn-Shaped bed profiles have two maximum scoured points which are located at both right and left lee sides of the

cylinder. In the case of Cone-Shaped bed profiles the maximum scoured point is located either in front of or beside the cylinder. The location of the maximum scoured point depends on the scour type, and we conclude therefore that this location can be applied to classify objectively the scour type. The maximum scoured point concept is applied for the following discussions.

To investigate the flow pattern near the bed around a cylinder, laboratory experiments were performed for several K.C. numbers. We observed that for low K.C. numbers, flow separation from the cylinder or a pair of symmetric vortices was generated, and this scoured the bed at the lee side of the cylinder. Finally, a Twin-Horn-Shaped scoured bed profile was formed. For large KC numbers, the Cone-Shaped scoured bed profiles were formed and an asymmetric vortex, similar to the Karman vortex appeared. Nishizawa *et al.* (1988) also observed the flow pattern under similar conditions. In general, our observations coincide with theirs. Except that they did not have any horseshoe vortex formation in any cases, even for the Cone-Shaped scored bed profile.

Based on these observations, we conclude that each scour type corresponds to a different flow pattern or vortex structures.

Figure 4 shows the relation of local scour type to the K.C. number. The

(a) Twin-Horn-Shaped

(b) Transient-Shaped

(c) Cone-Shaped

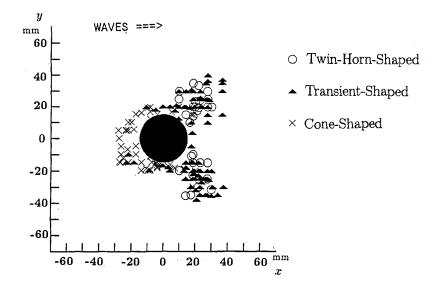FIG. 2. Typical Scour Bed Profiles

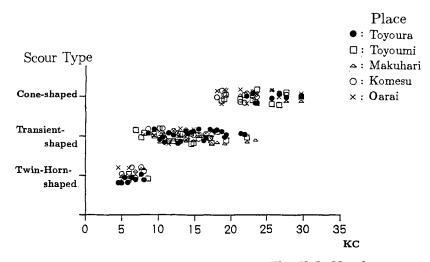FIG. 3.   Distribution of Maximum Scoured Points of All Experimental
Cases

FIG. 4.   Relation of Scour Type to The K.C. Number

ordinate in this figure indicates the scour type that is classified with the scoured bed profiles. From this figure it is clear that the flow pattern is well represented by the K.C. number. This relation has already been investigated (c.f. by Nishizawa and Sawamoto; 1988). The results reported by these authors and ours coincide in the following characteristics: the scour type changes from the Twin-Horn-Shaped to the Cone-Shaped as the K.C. number increases. The borders between the bed profiles Twin-Horn-Shaped and Transient-Shaped, as well as Transient-Shaped and Cone-Shaped are about 8.0 and 20.0 in K.C. number, respectively. These borders are independent of the sand diameter.

Figure 4 depicts the relation of scour type to the K.C. number. As the scour type is related to the flow pattern, represented by the K.C. number, and since the location of maximum scoured points are related to the scour types, as we showed previously, we conclude that the flow pattern can be explained in terms of the location of maximum scoured point.
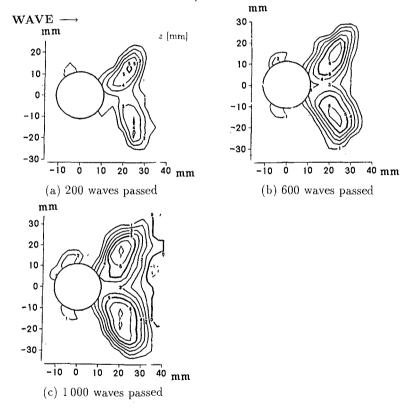

(a) 200 waves passed

(b) 600 waves passed

(c) 1 000 waves passed

FIG. 5.   Bottom Bed Profiles in The Local Scour Developing Process. (K.C. Number: 9.0, Scour Type: Twin-Horn-Shaped)

4. SCOUR DEVELOPING PROCESS

The time evolution of the local scour bed profiles around a cylinder was measured in 8 experimental cases. In the experiments, the range of the K.C. number varied from 4.38 to 30.9. The bottom bed profiles around the cylinder were measured every 200 waves passing the cylinder, until we considered that the bottom bed became almost stable. For all experimental cases, the initial bed was flat, and the scoured bed became almost stable after 1 000 waves passed the cylinder. The typical developing bed profiles measured are shown in Figs. 5 to 7. Figure 5 shows the Twin-Horn-Shaped scour type. Here, the bed at the lee side of the cylinder was scoured during each developing stage. The bed profiles after 200 and 600 waves passed the cylinder correspond to local scour developing stages. They show similar features to those of the profiles obtained after 1 000 waves

(a) 200 waves passed
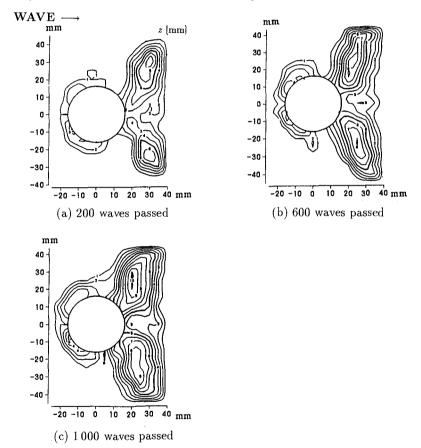
(b) 600 waves passed

(c) 1 000 waves passed

FIG. 6.   Bottom Bed Profiles in The Local Scour Developing Process. (K.C. Number: 11.0, Scour Type: Transient-Shaped)

passed, which is considered the equilibrium stage. The maximum scoured point remains located almost in the same place with respect to the cylinder, during every developing stage shown in this figure.

In Fig. 6 the Transient-Shaped scoured bed profile is depicted. This figure shows that the scouring develops at both the lee side of the cylinder and beside this one, during every developing stage. And, as in the case of the Twin-Horn Shaped bed profile, similar shape of bed scouring is retain during the whole developing procees.

Figure 7 shows the Cone-Shaped bed profile. Here as in the two previous cases, the scour shape found at the final equilibrium stage is the same that was formed during the earlier stages of the scour developing process. As mentioned in the previous section, the Cone-Shaped bed profile is associated with a horseshoe vortex, and the Twin-Horn-Shaped bed profile is with flow separation from the cylinder or a pair of separated vortices.

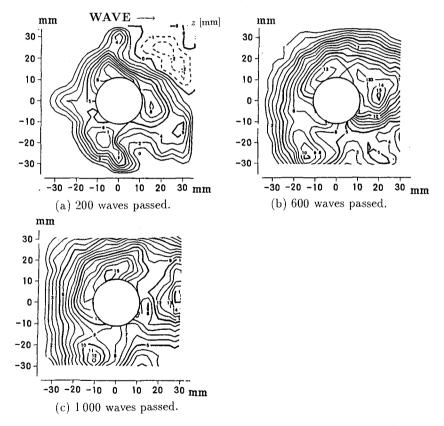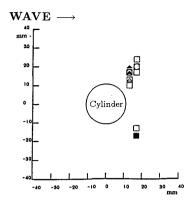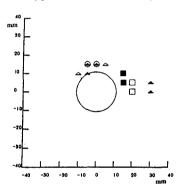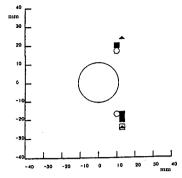No matter however what the flow pattern is, the respective scour bed

(a) 200 waves passed.   (b) 600 waves passed.

(c) 1 000 waves passed.

FIG. 7.   Bottom Bed Profiles in The Local Scour Developing Process. (K.C. Number: 30.9, Scour Type: Cone-Shaped)

WAVE $\longrightarrow$

(a) K.C. number : 9.0, Equilibrium
Scour Type : Twin-Horn-Shaped.

(b) K.C. number : 11.0, Equilibrium
Scour Type : Transient-Shaped.

○ : N = 200
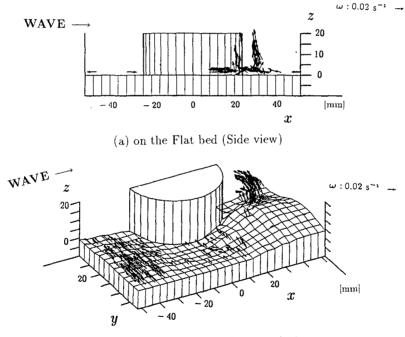
■ : N = 400

□ : N = 600

△ : N = 800

▲ : N = 1000

(c) K.C. number : 30.9, Equilibrium
Scour Type : Cone-Shaped.

FIG. 8. Location of Maximum Scoured Points in Each Developing Stage. N **Represents the Number of Waves That Passed The Cylinder.**

shapes appearing in the final equilibrium stage of the scour developing process is formed already at the earlier stages. This was confirmed in all experiments performed, and was found to be independent of the scour type.

Next, the developing process of local scour around a cylinder is discussed with the location of maximum scoured point. Figure 8 shows the distribution of maximum scoured points at each developing stage of local scouring for the cases corresponding to Figs. 5 to 7. The maximum scoured points in Figs. 8 (a) and (b) correspond to the cases of Twin-Horn-Shaped and the Transient-Shaped bed profiles, respectively. In both cases, these points are located at the right and left lee side of the cylinder, and they are apart from the cylinder contour. Fig. 8 (c) corresponds to the Cone-Shaped bed profile. Here, the maximum scoured points are located beside the cylinder. During the experiments performance, we observed

that in all cases the location of the maximum scoured points was almost fixed during the whole scouring process. We conclude therefore that the flow pattern near the bed around a cylinder is practically the same during all the local scouring developing process.

Kobayashi (1993) measured velocity distributions around a vertical cylinder on both flat bed and scoured bed, and computed the vorticity distribution shown in Fig. 9. In this figure, the phase θ is defined as 0 when a wave crest passes the cylinder axis, these vorticity distribution corresponds then to an instant just after the wave crest passes. Figures 9 (a) and (b) show the vorticity distribution in the initial and equilibrium stage of the developing process of local scouring, respectively. In Fig. 9 (a), the axis of the vortex formed apart from the cylinder contour is almost vertical and parallel to the cylinder axis. And in Fig. 9 (b) the vortex is deformed due to the scoured bed topography, and has an arch shape. From Figures 9 (a) and (b) this author concluded that the scoured bed profile changes the flow pattern near the bed around a cylinder, which contradicts the results obtained in this study. A reason for such contradiction may be attributed to the nonlinearity waves effect. This is because in Kobayashi (1993) study, non-

(a) on the Flat bed (Side view)

(b) on the Scoured bed (Perspective)

FIG. 9.   Vorticity Distribution Near The Bottom Around a Cylinder (Kobayashi, 1993) K.C. Number : 5.2, Phase θ : $\pi/4$

linearity of waves could be very important since Ursell number was 83.8. On the other hand, in this sudy linear waves were reproduced with maximum Ursell number of about 4. This is however just a supposition and studies to clarify the effect of nonlinearity of waves on the local scouring process are required.

5. ULTIMATE SCOUR DEPTH

The prediction of the ultimate local scour stage is very important for planning and maintenance of onshore and offshore structures. The predominat parameters in this ultimate stage are the depth and the scoured bed profile. The scoured bed profile has already been examined with the K.C. number. In this section, the local scour depth on the equilibrium stage is discussed.

   Figure 10 shows the relation of the ultimate scour depth to the K.C. number. The ordinate in this figure represents the maximum scour depth S divided by the cylinder diameter D. Six series of experimental results are shown in this figure. Five of them are results of this study, and one corresponds to experimental results obtained by Sumer et al. (1992). The solid line drawn in this figure indicates the relation evaluated empirically by these authors. Their experiments were performed on the live bed condition, and those of this study in clear water condition. In spite of this difference, most experimental results of this study agree well with the solid line. Only the results obtained for K.C. number less than 10 are in relative disagreement with this line; they show deeper maximum scour depths than the solid line does.

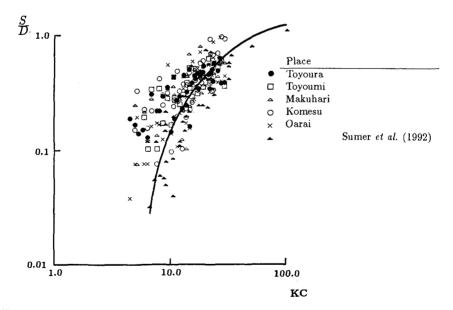   The scour bed profile for K.C. number less than 10 is of the Twin-Horn-

FIG. 10.   Relation Between Ultimate Scour Depth and K.C. Number

Shape type, as shown in Fig. 4. For this type of scour profile the maximum scoured points are located apart from the cylinder contour, as observed in Fig. 2(a) or 3. Since for engineering purposes, the local scour just at the vicinity of a cylinder is most serious than that apart from this, the maximum scour depth was reevaluated by considering a reduced area surrounding the cylinder, and excluding the maximum scoured points.

The results obtained after reevaluation are shown in Fig. 11. In this figure, the ordinate represents the ultimate scour depth on the vicinity of the cylinder surface S' divided by the cylinder diameter D. In Fig. 11 better agreement of the reevaluated results, for low K.C. numbers, with the solid line estimated by Sumer et al. (1992) is observed, comparing with Fig. 2 (a). From this results, we conclude that the maximum scour depth at the vicinity of the cylinder is related with the K.C. number, and is independent of the bed condition, live bed or clear water, as well as the sand diameter.

The reason why in the Twin-Horn-Shaped scoured bed the very near vicinity of the cylinder was not scoured is that, in this case the flow pattern did not show clear formation of the horseshoe vortex. Only flow separation on the lee side of the cylinder or a pair of separated vortices were visible. Sumer et al. (1992) reported that horseshoe vortices were abscent for K.C. numbers less than 6. and therefore the bed around the cylinder was not scoured under the live bed condition.

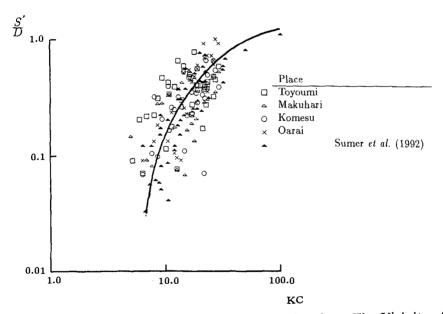Figure 12 shows the relation of the maximum scour depth in the ultimate

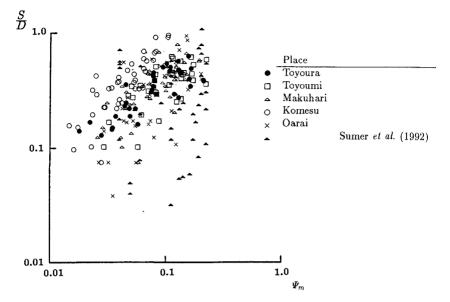FIG. 11.   Relation Between Ultimate Scour Depth on The Vicinity of The Cylinder surface and K.C. number

FIG. 12. Relation Between Ultimate Scoured Depth to Shields Parameter

stage to Shields parameter Ψ_m. The ordinate in this figure indicates the maximum scour depth in the ultimate stage S divided by the cylinder diameter D. The Shields parameter Ψ_m is calculated from the incident wave conditions shown in Table 1, and the sand characteristics listed in Table 2. In Fig. 12 the relation of the maximum scour depth to the Shields parameter is shown. We observe here that the maximum scour depth has a poor relation with the Shields parameter.

6. CONCLUSIONS

In this sudy, local scour around a vertical cylinder and its developing process were investigated experimentally with the flow pattern near the bed. Local scoured bed profiles were classified into the types: Twin-Horn-Shaped, Transient-Shaped and Cone-Shaped. The location of the maximum scoured points was introduced to classify objectively the bed profiles. This location was found to be related to the flow pattern near the bed around the cylinder. In the case of Twin-Horn-Shaped scoured bed profile a pair of maximum scoured points are located at the right and left lee side of the cylinder, and they are apart from the cylinder contour. This type of bed profile is associated with the formation of flow separation or a pair of separated vortices. In the case of the Cone-Shaped scoured bed profile, one maximum scoured point is found, and this is located in front or beside the cylinder. During the whole local scour developing process the bed profiles have a similar shape, and the location of the maximum scoured point or points is almost fixed. These features are independent of the scour type. Finally, we found that

the maximum scour depth has a close relation to the K.C. number, and a very poor relation to the Shields parameter . Also that, this depth is independent of the bottom bed condition, live bed or clear water, and the sand diameter.

REFERENCES

Kobayashi, T (1993): "3-D analysis of flow around a vertical cylinder on a scoured bed." *Proc. 23rd Int. Conf. on Coastal Engrg.*, ASCE, Vol. 3, pp.3482–3495.

Nishizawa, M., M. Minami and M. Sawamoto (1988): "Relation of the flow pattern to local scour around a vertical cylinder in wave field." *Proc. of 43rd Conf. of JSCE*, II, pp.758-759 (in Japanese).

Nishizawa, M. and M. Sawamoto (1988): "Local scour around a vertical cylinder under the wave action." *Proc. of the 6th Congress of APD–IAHR*, pp.121–128.

Sumer, B. Mutlu, J. Fredsøe, and N. Christiansen (1992): "Scour around vertical pile in waves." *Jour. Waterways, Port, Coastal, and Ocean Engrg.*, ASCE, Vol. 118, No.1, pp.15–31.

Wells, D. R. and R. M. Sorensen (1970): "Scour around a circular cylinder due to wave motion." *Proc. of the 12th Coastal Eng. Conf.*, pp.1263–1279.